RESEARCH PAPER

PCCP
www.rsc.org/pccp

Infrared emission spectra and equilibrium bond lengths of gaseous ZnH_2 and ZnD_2†

Alireza Shayesteh,[a] Iouli E. Gordon,[b] Dominique R. T. Appadoo[ac] and Peter F. Bernath*[ab]

[a] *Department of Chemistry, University of Waterloo, 200 University Avenue West, Waterloo, ON, Canada N2L 3G1. E-mail: bernath@uwaterloo.ca; Fax: +1-519-746-0435; Tel: +1-519-888-4814*

[b] *Department of Physics, University of Waterloo, 200 University Avenue West, Waterloo, ON, Canada N2L 3G1*

[c] *Canadian Light Source Inc., University of Saskatchewan, 101 Perimeter Road, Saskatoon, SK, Canada S7N 0X4*

Received 27th May 2005, Accepted 6th July 2005
First published as an Advance Article on the web 20th July 2005

A detailed analysis of the high resolution infrared emission spectra of gaseous ZnH_2 and ZnD_2 in the 800–2200 cm^{-1} spectral range is presented. The ν_3 antisymmetric stretching fundamental bands of $^{64}ZnH_2$, $^{66}ZnH_2$, $^{67}ZnH_2$, $^{68}ZnH_2$, $^{64}ZnD_2$, $^{66}ZnD_2$ and $^{68}ZnD_2$, as well as several hot bands involving ν_1, ν_2 and ν_3 were rotationally analyzed, and spectroscopic constants were obtained. Rotational *l*-type doubling and *l*-type resonance, local perturbations, and Fermi resonances were observed in the vibration–rotation bands of both ZnH_2 and ZnD_2, and equilibrium vibrational frequencies (ω_1, ω_2 and ω_3) were estimated. Using the rotational constants of the 000, 100, 01^10 and 001 vibrational levels, the equilibrium rotational constants (B_e) of $^{64}ZnH_2$ and $^{64}ZnD_2$ were determined to be 3.600 269(31) cm^{-1} and 1.801 985(25) cm^{-1}, respectively, and the associated equilibrium bond lengths (r_e) are 1.524 13(1) Å and 1.523 94(1) Å, respectively. The difference between the r_e values of $^{64}ZnH_2$ and $^{64}ZnD_2$ is about 0.01%, and is mainly due to the breakdown of the Born–Oppenheimer approximation.

1. Introduction

Solid ZnH_2 has been known since 1951, and several methods have been reported for its synthesis.[1–8] Chemical properties of solid ZnH_2, as well as its infrared absorption spectrum and the X-ray diffraction pattern were studied in the 1970s.[6–8] Recently, Wang and Andrews[9] recorded the infrared spectra of solid ZnH_2 and ZnD_2, and observed broad absorption bands characteristic of hydrogen-bridge bonding. Solid ZnH_2 decomposes to the constituent elements at 90 °C,[4] and it is not possible to produce gaseous ZnH_2 by heating the solid. The lack of stability of solid ZnH_2 has been further confirmed by theoretical calculations.[10] Linney and Russell found that ZnH_2 can be generated by the infrared laser pyrolysis of diethylzinc.[11] The reduction of aqueous Zn(II) in acidic solutions with $NaBH_4$ results in formation of a volatile zinc-containing compound. This molecule has not been identified yet, but it might be zinc dihydride.[12,13] Properties of the main-group metal hydrides, including hydrides of group 11 and 12 elements, have been reviewed by Aldridge and Downs.[14]

There have been a few *ab initio* theoretical studies on electronic structure and geometry of gaseous ZnH_2.[15–21] A linear H–Zn–H structure and a closed-shell $\tilde{X}^1\Sigma_g^+$ ground electronic state have been predicted by all theoretical calculations. The Zn–H bond distances estimated by various theoretical models[15–21] were in the range of 1.492 to 1.662 Å. Vibrational frequencies of ZnH_2, ZnHD and ZnD_2 were calculated by Greene *et al.* at the MP2 and CCSD(T) levels of theory with relatively large basis sets.[21] It was also calculated that the gas phase reaction: Zn (g) + H_2 (g) → ZnH_2 (g) is endoergic by only a few kcal mol^{-1} for ground state (^{1}S) zinc atoms.[21] The metastable ^{3}P state of Zn, which is the first excited state, lies about 93 kcal mol^{-1} above the ground state[22] so the production of gaseous ZnH_2 from the gas phase reaction of Zn(^{3}P) with H_2 is highly exoergic.

The gas phase reaction of excited zinc atoms with molecular hydrogen has been studied extensively, both by theoretical calculations and by laser pump–probe techniques.[23–29] Although the ground state Zn(^{1}S) does not react with H_2 due to a high energy barrier, excited zinc atoms in ^{3}P or ^{1}P states can insert into the H–H bond.[23–29] The resultant intermediate is an excited bent [H–Zn–H]* complex, which can dissociate to ZnH and H free radicals. All theoretical and experimental studies on this reaction[23–29] considered ZnH and H as the only products, and no attention was given to the possible formation of the ground state linear H–Zn–H molecule. The activation of H–H bond with excited Mg, Zn, Cd and Hg atoms has been reviewed by Breckenridge.[29]

Matrix isolation, followed by infrared absorption spectroscopy, has been used to study many metal hydrides.[30] The ZnH_2, ZnHD and ZnD_2 molecules were formed in solid argon and krypton matrices at ~12 K from the reaction of excited zinc atoms with hydrogen.[21,31] Infrared absorption spectra of these species (trapped in solid matrices) were recorded, and vibrational frequencies for the antisymmetric stretching (ν_3) and bending (ν_2) modes were obtained. Wang and Andrews[9] have recently repeated this experiment using solid hydrogen and neon matrices at 4.5 K, and recorded the infrared absorption spectra of several zinc hydride species at a relatively high resolution. ZnH_2 has also appeared as a byproduct in the matrix isolation experiments studying the reactions of Zn with SiH_4, HCl and H_2O.[32–34]

We have recently reported the first observation of ZnH_2, CdH_2 and HgH_2 molecules in the gas phase.[35–37] The molecules were generated by the reactions of metal vapor with molecular hydrogen in the presence of an electrical discharge.

† Electronic supplementary information (ESI) available: A complete list of the observed line positions and the outputs of least-squares fitting program (Tables S1–S13). See http://dx.doi.org/10.1039/b507539d

DOI: 10.1039/b507539d

Gaseous ZnH_2, CdH_2 and HgH_2 were unambiguously identified by their high resolution infrared emission spectra, and the ν_3 fundamental bands were rotationally analyzed to determine the r_0 metal–hydrogen bond distances.[35–37] The only other metal dihydrides observed in the gas phase are FeH_2, BeH_2 and MgH_2.[38–44] A complete analysis of all the vibration–rotation bands observed in the infrared emission spectra of gaseous ZnH_2 and ZnD_2 is presented in this paper.

2. Experiment and results

Gaseous ZnH_2 and ZnD_2 were generated in a furnace-discharge emission source, which was described in detail in our earlier papers.[35,36] Zinc rods were placed inside an alumina tube and heated to 470 °C. The tube contained two stainless-steel electrodes, and was evacuated using a rotary pump. Pure hydrogen or deuterium (0.5–2.5 Torr) flowed slowly through the tube, and a dc discharge was created between the electrodes. The emission from the tube was focused onto the entrance aperture of a Bruker IFS 120 HR Fourier transform spectrometer. Emission spectra were recorded using a KBr beamsplitter and a HgCdTe (MCT) detector, cooled by liquid nitrogen. The spectrum of ZnH_2 was recorded in the 1200–2200 cm^{-1} spectral range using a 2200 cm^{-1} long-wave pass filter, and the instrumental resolution was set to 0.01 cm^{-1}. In order to improve the signal-to-noise ratio, 200 scans were co-added during three hours of recording. The spectrum of ZnD_2 was recorded in the 800–1600 cm^{-1} spectral range using a 1600 cm^{-1} long-wave pass filter. The instrumental resolution was 0.01 cm^{-1}, and 400 scans were co-added. The signal-to-noise ratios for the strongest emission lines of ZnH_2 and ZnD_2 were about 50 and 20, respectively.

In addition to atomic and molecular emission lines, the spectra contained blackbody emission from the hot tube and absorption lines due to atmospheric water vapor. The blackbody emission profile was subtracted from the spectra, in order to obtain flat baselines. Molecular emission lines due to vibration–rotation transitions of ZnH, ZnH_2, CO, ZnD and ZnD_2 were identified. Line positions were measured using the WSPECTRA program written by M. Carleer (Université Libre de Bruxelles). Emission lines of CO appeared in the ZnH_2 spectrum, and were used for absolute wavenumber calibration.[45] The calibration factor for ZnD_2 spectrum was determined using thirteen strong atomic lines common to the ZnH_2 and ZnD_2 spectra. The absolute accuracy of our calibrated line positions is better than 0.001 cm^{-1}. Assignment of the vibration–rotation bands was facilitated using a color Loomis-Wood program.

An overview of the ZnH_2 spectrum is shown in Fig. 1. Zinc has five stable isotopes, and their terrestrial abundances are: ^{64}Zn (48.6%), ^{66}Zn (27.9%), ^{67}Zn (4.1%), ^{68}Zn (18.8%), and ^{70}Zn (0.6%). Lines from different isotopes of zinc were completely resolved in both spectra, and their intensity ratios match their natural abundances. The adjacent rotational lines in ZnH_2 and ZnD_2 spectra had 3 : 1 and 1 : 2 intensity ratios, respectively, due to the *ortho–para* nuclear spin statistical weights associated with hydrogen ($I = 1/2$) and deuterium ($I = 1$) nuclei.[46] An expanded view of the ZnD_2 spectrum in Fig. 2 shows the 1 : 2 intensity alternation. In addition to the ν_3 fundamental band, *i.e.*, 001 (Σ_u^+) → 000 (Σ_g^+), the following hot bands were assigned for the most abundant isotopologues, $^{64}ZnH_2$ and $^{64}ZnD_2$:

002 (Σ_g^+) → 001 (Σ_u^+), 003 (Σ_u^+) → 002 (Σ_g^+),
101 (Σ_u^+) → 100 (Σ_g^+), 01^11 (Π_g) → 01^10 (Π_u),
02^21 (Δ_u) → 02^20 (Δ_g), 02^01 (Σ_u^+) → 02^00 (Σ_g^+).

The 004 (Σ_g^+) → 003 (Σ_u^+) band of $^{64}ZnH_2$ and the 01^12 (Π_u) → 01^11 (Π_g) band of $^{64}ZnD_2$ were also found. Fewer hot bands were detectable for the ^{66}Zn and ^{68}Zn isotopes because of their lower abundances. Lines from the ^{67}Zn and ^{70}Zn isotopes were too weak to be observed, except for the 001 (Σ_u^+) → 000 (Σ_g^+) fundamental band of $^{67}ZnH_2$. We were also able to assign the

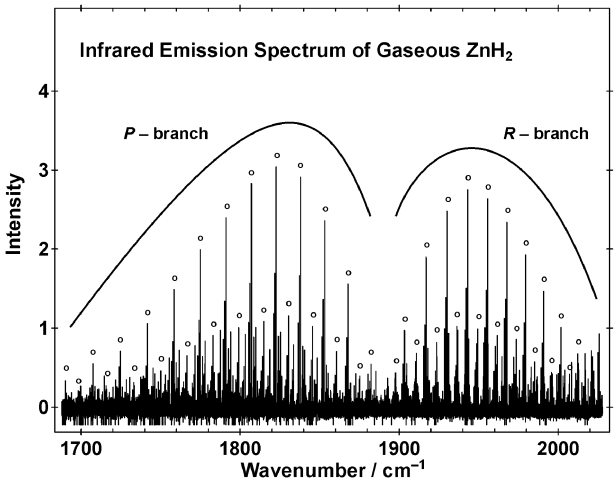

Fig. 1 An overview of the infrared emission spectrum of gaseous ZnH_2. The strongest emission lines with 3 : 1 intensity alternation are from the antisymmetric stretching fundamental band. The lines above 2000 cm^{-1} are mostly from CO.

200 (Σ_g^+) → 001 (Σ_u^+) combination band for the $^{64}ZnH_2$, $^{66}ZnH_2$ and $^{68}ZnH_2$ isotopologues. An approximate energy level diagram showing all the observed vibration–rotation bands of $^{64}ZnH_2$ is drawn in Fig. 3.

3. Data analysis

3.1. Σ → Σ and Π → Π transitions

The total energy of a linear triatomic molecule in its ground electronic state can be separated into vibrational and rotational parts:

$$E_{\text{vib–rot}} = G(v_1, v_2^l, v_3) + F_{[v]}(J). \quad (1)$$

The vibrational energy expression includes first-order harmonic and second-order anharmonic terms:[46]

$$\begin{aligned} G(v_1, v_2^l, v_3) =& \omega_1\left(v_1 + \tfrac{1}{2}\right) + \omega_2(v_2 + 1) + \omega_3\left(v_3 + \tfrac{1}{2}\right) \\ &+ x_{11}\left(v_1 + \tfrac{1}{2}\right)^2 + x_{22}(v_2 + 1)^2 + x_{33}\left(v_3 + \tfrac{1}{2}\right)^2 \\ &+ g_{22}l^2 + x_{12}\left(v_1 + \tfrac{1}{2}\right)(v_2 + 1) \\ &+ x_{13}\left(v_1 + \tfrac{1}{2}\right)\left(v_3 + \tfrac{1}{2}\right) + x_{23}(v_2 + 1)\left(v_3 + \tfrac{1}{2}\right). \end{aligned} \quad (2)$$

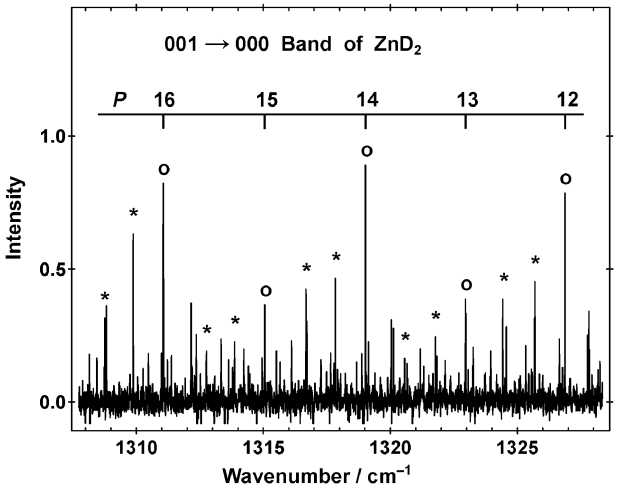

Fig. 2 An expanded view of the ZnD_2 spectrum showing the isotope splitting and the 1 : 2 intensity alternation in *P*-branch lines of the ν_3 fundamental band. The lines marked with circles are from $^{64}ZnD_2$, and those marked with stars are from $^{66}ZnD_2$ and $^{68}ZnD_2$. The weaker lines (unmarked) are from the hot bands of ZnD_2.

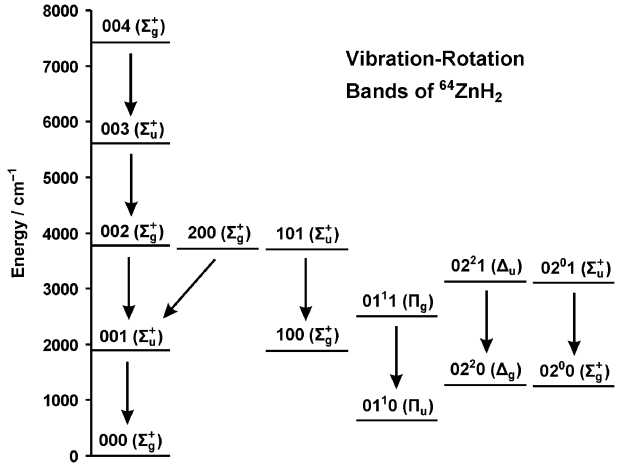

Fig. 3 An approximate energy level diagram showing the observed vibration–rotation bands of $^{64}ZnH_2$ in the ν_3 region.

In this equation, v_1, v_2 and v_3 are the vibrational quantum numbers for the symmetric stretching (σ_g), bending (π_u), and antisymmetric stretching (σ_u) modes, respectively, and l is the vibrational angular momentum quantum number. For the vibrational states with $\Sigma(l = 0)$ or $\Pi(l = 1)$ symmetry, the following expression was used for rotational energy levels:[47]

$$F_{[v]}(J) = B[J(J+1) - l^2] - D[J(J+1) - l^2]^2 + H[J(J+1) - l^2]^3 \pm \frac{1}{2}[qJ(J+1) + q_D J^2(J+1)^2]. \quad (3)$$

B is the inertial rotational constant, D and H are centrifugal distortion constants, and J is the total angular momentum quantum number (including rotation). The rotational l-type doubling parameters, q and q_D, are zero for the Σ states, and the $+(-)$ sign refers to e (f) parity component of the Π states.[48] We used an experimental uncertainty of 0.001 cm^{-1} for lines from the 001 → 000, 002 → 001 and 01^11 → 01^10 bands of ZnH_2 and ZnD_2. Lines from the other hot bands were less intense, and were given an uncertainty of 0.002 cm^{-1}.

The absolute rotational assignments of the 001 (Σ_u^+) → 000 (Σ_g^+) fundamental bands of ZnH_2 and ZnD_2 were easily obtained because we observed all the rotational lines near the band origins. The intensity alternations in adjacent rotational lines and small local perturbations at high J's of the 001 (Σ_u^+) state of both ZnH_2 and ZnD_2 further confirmed our absolute J assignments. The local perturbations observed in the 001 level are caused by the nearby 030 level, because both theoretical calculations[21] and matrix isolation experiments[21,31] had found that the frequency of the antisymmetric stretching mode is close to three times the frequency of the bending mode, *i.e.*, $\nu_3 \approx 3\nu_2$. Rotational lines of the 001 (Σ_u^+) → 000 (Σ_g^+) fundamental bands were fitted using the energy expression in eqn. (3), and the ground state vibrational energy was set to zero. For the perturbed rotational levels in the 001 (Σ_u^+) state, *i.e.*, $J' > 15$ for ZnH_2 and $J' > 20$ for ZnD_2, the total energies were fitted to term values. As a result, accurate rotational constants were obtained for the 000 ground states of ZnH_2 and ZnD_2, while the rotational constants of the 001 states can reproduce the data only for the lower J's.

The rotational assignment of the 002 (Σ_g^+) → 001 (Σ_u^+), 003 (Σ_u^+) → 002 (Σ_g^+) and 004 (Σ_g^+) → 003 (Σ_u^+) hot bands were obtained consecutively using lower state combination differences. The 002 (Σ_g^+) states of both ZnH_2 and ZnD_2 were globally perturbed by the nearby 200 (Σ_g^+) states. The *ab initio* calculations of Greene *et al.*[21] have predicted that ν_1 and ν_3 are nearly equal in frequency. The 001 and 100 levels have opposite g/u symmetry and do not interact with each other. However, the 002 and 200 levels both have Σ_g^+ symmetry and are strongly coupled by Fermi resonance. Due to the strong mixing of the 002 and 200 levels in ZnH_2, rotational lines of the 200 (Σ_g^+) → 001 (Σ_u^+) combination band of ZnH_2 appeared in our spectrum, and were easily assigned using lower state combination differences. The energy expression in eqn. (3) was used for all these vibrational levels, and effective spectroscopic constants were determined for all the observed isotopologues. A complete list of the observed line positions and the outputs of our least-squares fitting program have been placed in Tables S1–S7, provided as electronic supplementary information (ESI).† Effective spectroscopic constants for several vibrational states of $^{64}ZnH_2$ and $^{64}ZnD_2$ are presented in Tables 1 and 2, respectively, and those for the minor isotopologues are in Table S8. The total energies of high J levels of the 001 (Σ_u^+) states were fitted as term values, and the values are presented in Tables S1–S7. The effect of Fermi resonance was neglected in determination of constants of Tables 1 and 2, but the effective constants reported in these tables can reproduce the data within the experimental uncertainty (0.001 or 0.002 cm^{-1}).

The second strongest bands in both ZnH_2 and ZnD_2 spectra had large l-type doubling, and were assigned as the 01^11 (Π_g) → 01^10 (Π_u) hot bands. The absolute J assignment for these bands were obtained based on the intensity alternations and the fact that e and f parity components must have the same

Table 1 Effective spectroscopic constants (in cm^{-1}) for the Σ and Π vibrational states of $^{64}ZnH_2$

State	$G_{[v]} - G_{000}$	B	$D/10^{-5}$	$H/10^{-10}$	$q/10^{-2}$	$q_D/10^{-6}$
000 (Σ_g^+)	0.0	3.548 2143(86)[a]	4.9225(25)	4.27(22)		
001 (Σ_u^+)[b]	1889.433 10(24)	3.506 5650(83)	4.9001(23)			
002 (Σ_g^+)[c]	3772.292 98(33)	3.457 8091(65)	4.7293(10)			
200 (Σ_g^+)[c]	3712.969 42(60)	3.451 241(15)	5.0353(57)			
003 (Σ_u^+)	5605.283 50(56)	3.419 5915(88)	4.8433(19)			
004 (Σ_g^+)	7422.500 30(75)	3.372 528(12)	4.6570(31)			
01^10 (Π_u)[d]	ν_2	3.542 900(10)	4.9850(18)		−5.9464(21)	2.920(35)
01^11 (Π_g)	1876.966 90(24) + ν_2	3.501 569(11)	4.9792(21)		−5.8509(21)	2.784(41)
100 (Σ_g^+)[d]	ν_1	3.496 356(27)	4.8994(77)			
101 (Σ_u^+)	1827.656 21(46) + ν_1	3.454 273(27)	4.9321(77)			

[a] The numbers in parentheses are one standard deviation statistical uncertainties in the last quoted digits. [b] The effective constants of the 001 state can accurately reproduce the $J = 0$ to 15 rotational energy levels (see the text). [c] The effect of Fermi resonance between the 002 and 200 states was neglected in determination of these constants (see the text). [d] The wavenumbers of ν_1 and ν_2 could not be determined from our data. The neon matrix value (ref. 9) for ν_2 is 632.5 cm^{-1}, and ν_1 is almost equal to ν_3.

Table 2 Effective spectroscopic constants (in cm^{-1}) for the Σ and Π vibrational states of $^{64}ZnD_2$

State	$G_{[v]} - G_{000}$	B	$D/10^{-5}$	$H/10^{-10}$	$q/10^{-2}$	$q_D/10^{-6}$
000 (Σ_g^+)	0.0	1.783 4239(67)[a]	1.2271(11)	0.452(54)		
001 (Σ_u^+)[b]	1371.631 34(22)	1.767 9889(64)	1.220 73(93)			
002 (Σ_g^+)[c]	2732.322 43(32)	1.752 1750(56)	1.215 09(56)			
003 (Σ_u^+)	4076.865 17(57)	1.736 6911(64)	1.215 86(68)			
01^10 (Π_u)[d]	ν_2	1.781 7330(48)	1.237 46(38)		−2.0744(10)	0.491(8)
01^11 (Π_g)	1364.992 38(19) + ν_2	1.766 3714(50)	1.234 01(48)		−2.0538(10)	0.466(9)
01^12 (Π_u)	2719.380 19(44) + ν_2	1.750 5663(57)	1.229 74(60)		−2.0353(10)	0.467(10)
100 (Σ_g^+)[d]	ν_1	1.765 108(27)	1.2215(52)			
101 (Σ_u^+)	1340.310 10(52) + ν_1	1.749 586(28)	1.2278(55)			

[a] The numbers in parentheses are one standard deviation statistical uncertainties in the last quoted digits. [b] The effective constants of the 001 state can accurately reproduce the $J = 0$ to 20 rotational energy levels (see the text). [c] The effect of Fermi resonance between the 002 and 200 states was neglected in determination of these constants (see the text). [d] The wavenumbers of ν_1 and ν_2 could not be determined from our data. The neon matrix value (ref. 9) for ν_2 is 456.4 cm^{-1}, and ν_1 is about 30 cm^{-1} smaller than ν_3.

band origins. Small local perturbations were observed in the high J's of the 01^11 (Π_g) state for both ZnH_2 and ZnD_2. These perturbations are caused by the nearby 040 vibrational level, and they further confirmed our absolute J numbering. Rotational lines of the 01^11 (Π_g) → 01^10 (Π_u) bands were fitted using the energy expression in eqn. (3) with $l = 1$. For the perturbed rotational levels in the 01^11 (Π_g) state, the total energies were fitted to term values. The vibrational energy of the 010 level was set to zero, since we can only determine the difference between 01^11 and 01^10 vibrational energies with our data. The rotational assignment of the 01^12 (Π_u) → 01^11 (Π_g) hot band of ZnD_2 was easily obtained using lower state combination differences. Rotational constants and the l-type doubling constants of the 01^10, 01^11 and 01^12 states are reported in Tables 1 and 2 for $^{64}ZnH_2$ and $^{64}ZnD_2$, respectively. The corresponding constants for the minor isotopes of zinc and the total energies of high J levels of the 01^11 (Π_g) states (term values) are presented in Tables S1–S6.†

Knowing the rotational constants (B) of the 000, 01^10 and 001 levels, we calculated the vibration–rotation interaction constants, α_2 and α_3, of $^{64}ZnH_2$ and $^{64}ZnD_2$ using the following linear equation:[46]

$$B_{[v]} = B_e - \alpha_1\left(v_1 + \tfrac{1}{2}\right) - \alpha_2(v_2 + 1) - \alpha_3\left(v_3 + \tfrac{1}{2}\right). \quad (4)$$

The equilibrium Zn–H and Zn–D bond distances (r_e) must be equal within the Born–Oppenheimer approximation, and therefore, the ratio of B_e values for $^{64}ZnH_2$ and $^{64}ZnD_2$ is simply given by:

$$\frac{B_e(^{64}ZnH_2)}{B_e(^{64}ZnD_2)} = \frac{m_D}{m_H} \quad (5)$$

where m_D and m_H are atomic masses of deuterium and hydrogen, respectively. Similarly, using the explicit expressions given for α_1 in symmetric linear triatomic molecules,[47,49,50] we found that the following relationship exists for this vibration–rotation interaction constant:

$$\frac{\alpha_1(^{64}ZnH_2)}{\alpha_1(^{64}ZnD_2)} = \left(\frac{m_D}{m_H}\right)^{3/2}. \quad (6)$$

Using the B_{000}, α_2 and α_3 constants of $^{64}ZnH_2$ and $^{64}ZnD_2$, we estimated the values of α_1 and B_e for these isotopologues by taking advantage of their isotopic ratios, eqns. (4)–(6). The absolute J assignments of the 101 (Σ_u^+) → 100 (Σ_g^+) hot bands of ZnH_2 and ZnD_2 were obtained immediately, because we had reasonable estimates for α_1 constants. The observed rotational levels of this band were not perturbed, and all the lines were fitted using the energy expression in eqn. (3). Similar to the 01^11 (Π_g) → 01^10 (Π_u) hot band, the unknown vibrational energy of the lower state (100, Σ_g^+) was set to zero in the least-squares fitting (see Tables 1 and 2).

3.2. Rotational *l*-type resonance

The 02^21 (Δ_u) → 02^20 (Δ_g) hot bands of $^{64}ZnH_2$ and $^{64}ZnD_2$ were rotationally assigned using the α_2 values determined in the previous section. The f parity levels of the Δ states ($l = 2$) were not perturbed, and a simple energy level expression similar to eqn. (3) was used to fit this sub-band:

$$E_\Delta^0 = G_\Delta + B_\Delta\,[J(J+1) - 4] - D_\Delta\,[J(J+1) - 4]^2. \quad (7)$$

However, the Δ state levels with e parity are shifted to higher energies due to an interaction with the nearby Σ^+ states (e parity). The vibrational energies of the 02^00 (Σ_g^+) and 02^01 (Σ_u^+) states are slightly smaller than those of 02^20 (Δ_g) and 02^21 (Δ_u) states, respectively, and the difference is equal to $4g_{22}$ (see eqn. (2)). The interaction between Σ^+ (e) and Δ (e) states of a degenerate vibrational level is due to rotational l-type resonance.[51,52] Following Maki and Lide,[52] we used a 2 × 2 Hamiltonian matrix to fit the Σ^+ (e) and Δ (e) states energy levels:

$$\boldsymbol{H} = \begin{pmatrix} E_\Sigma^0 & \sqrt{2}W_{20} \\ \sqrt{2}W_{20} & E_\Delta^0 \end{pmatrix}. \quad (8)$$

In this equation, E_Δ^0 is the same as that in eqn. (7), and the other two matrix elements are given by the following equations in which $x = J(J+1)$:

$$E_\Sigma^0 = (G_\Delta - 4g_{22}) + B_\Sigma J(J+1) - D_\Sigma\,[J(J+1)]^2, \quad (9)$$

$$W_{20} = \frac{1}{\sqrt{2}}(q + q_D x)[x(x-2)]^{1/2}. \quad (10)$$

For both $^{64}ZnH_2$ and $^{64}ZnD_2$ molecules, the 02^21 (Δ_u) → 02^20 (Δ_g) and 02^01 (Σ_u^+) → 02^00 (Σ_g^+) hot bands were fitted simultaneously using eqns. (7)–(10), and the constants of Tables 3 and 4 were obtained. Like the other hot bands, the unknown vibrational energies of the lower states, *i.e.*, $G(02^20)$, were set to zero and the band origins, $[G(02^21) - G(02^20)]$, were determined. The l-type doubling constants (q and q_D) of the 020 level are very close to those of the 01^10 (Π_u) state, and the off-diagonal matrix element of eqn. (8) changes from zero (at $J = 0$ and 1) to about −27 cm^{-1} for $^{64}ZnH_2$ (at $J = 21$) and −15 cm^{-1} for $^{64}ZnD_2$ (at $J = 27$). We also found that the fitted values of B_Δ and D_Δ in Tables 3 and 4 remain unchanged if we fit only the Δ states f levels. For the minor isotopologues, $^{66}ZnH_2$ and $^{66}ZnD_2$, only the f component of the 02^21 (Δ_u) → 02^20 (Δ_g) band was found and analyzed using eqn. (7), and the constants are listed in Table S8.†

The g_{22} constants for the 020 vibrational levels of $^{64}ZnH_2$ and $^{64}ZnD_2$ were found to be 5.381(6) cm^{-1} and 2.649(5) cm^{-1},

Table 3 Spectroscopic constants (in cm^{-1}) for the observed rotational *l*-type resonance in $^{64}ZnH_2$

	State	B	$D/10^{-5}$	g_{22}	$q/10^{-2}$	$q_D/10^{-6}$	$G(02^21) - G(02^20)$
020	02^20 (Δ_g)	3.537 760(24)[a]	5.0845(41)	5.3811(59)	−5.9478(58)	2.606(97)	
	02^00 (Σ_g^+)	3.539 000(51)	5.079(11)				
							1864.550 42(57)
021	02^21 (Δ_u)	3.496 783(25)	5.0906(44)	5.3386(58)	−5.8508(57)	2.467(93)	
	02^01 (Σ_u^+)	3.497 946(49)	5.071(11)				

[a] All uncertainties are 1σ.

respectively. In our previous work on BeH_2 and BeD_2,[42] we determined the g_{22} constants by calculating the difference between the 02^00 (Σ_g^+) and 02^20 (Δ_g) vibrational energies and dividing it by a factor of 4. Since we had used an effective energy level expression without the l^2 term for the Δ states of BeH_2 and BeD_2, instead of eqn. (7), the $[-B_\Delta l^2]$ term had been added to the vibrational energies of the Δ states. Therefore, the effective g_{22} constants of 2.050(1) cm^{-1} and 0.150(2) cm^{-1} reported for BeH_2 and BeD_2 in ref. 42 are in fact equal to $[g_{22} - B_\Delta]$, and should not be directly compared with those of $^{64}ZnH_2$ and $^{64}ZnD_2$. If one uses eqn. (7) for BeH_2 and BeD_2, the resultant g_{22} values will be 6.772(1) cm^{-1} and 2.524(2) cm^{-1}, respectively.

3.3. Local perturbations

For both $^{64}ZnH_2$ and $^{64}ZnD_2$ molecules, high rotational levels of the 001 (Σ_u^+) state are perturbed by the nearby 030 vibrational level, which has 03^10 (Π_u) and 03^30 (Φ_u) states. Rotational levels of the 001 (Σ_u^+) state of ZnH_2 with $J \leq 17$ are shifted towards higher energies, whereas the $J \geq 18$ levels are shifted towards lower energies. Similarly, the rotational levels of the 001 (Σ_u^+) state of ZnD_2 with $J \leq 22$ were shifted up and the $J \geq 23$ levels were shifted down. The magnitudes of these perturbations were small, and the largest energy shifts were about 0.04 cm^{-1}, observed right at the crossing point ($J = 17$ for ZnH_2 and $J = 22$ for ZnD_2). The perturbation pattern observed in both ZnH_2 and ZnD_2 clearly indicates that the perturbing state has a larger effective $B_{[v]}$ value. We estimated the effective $B_{[v]}$ values of the 03^10 (Π_u) and 03^30 (Φ_u) states using the $B_{[v]}$ values of the 000, 01^10, 02^00 and 02^20 states. The 03^10 (Π_u) and 03^30 (Φ_u) states have *e* and *f* parity components, but only the *e* parity levels can interact with the 001 (Σ_u^+) rotational levels. Due to the large rotational *l*-type doubling in the 03^10 (Π_u) state, the effective $B_{[v]}$ value of its *e* parity component becomes considerably smaller than that of the 001 (Σ_u^+) state. Therefore, in both ZnH_2 and ZnD_2, the 03^30 (Φ_u) state is responsible for the observed perturbations in the 001 (Σ_u^+) state. We constructed a 3×3 Hamiltonian matrix for the *e* parity levels of 001 (Σ_u^+), 03^30 (Φ_u), and 03^10 (Π_u) states. The 03^10 (Π_u) state was included in the matrix because it interacts with the 03^30 (Φ_u) state through rotational *l*-type resonance,[52] and thus has an indirect effect on the state of interest (001, Σ_u^+). The vibrational energy difference between the 03^10 and 03^30 states is equal to $8g_{22}$ (see eqn. (2)). Maki and Lide[52] have derived the Hamiltonian matrix for rotational *l*-type resonance between Π and Φ states. After parity transformation and including the Σ_u^+ (*e*) state, we obtained the following 3×3 Hamiltonian matrix for the *e* levels:

$$\boldsymbol{H} = \begin{pmatrix} E_\Sigma^0(001) & -W_{03} & 0 \\ -W_{03} & E_\Phi^0 & W_{31} \\ 0 & W_{31} & E_\Pi^0 + W_{11} \end{pmatrix}. \quad (11)$$

The matrix element connecting the Σ_u^+ and Π_u states was fixed to zero because we knew that the Φ_u state is causing the perturbation in the 001 (Σ_u^+) state. The following expressions, in which $x = J(J + 1)$, were used for the above matrix elements:

$$E_\Sigma^0(001) = G_{001} + B_{001}J(J+1) - D_{001}[J(J+1)]^2 + H_{001}[J(J+1)]^3 \quad (12)$$

$$E_\Phi^0 = G_\Phi + B_\Phi[J(J+1) - 9] - D_\Phi[J(J+1) - 9]^2 \quad (13)$$

$$E_\Pi^0 = (G_\Phi - 8g_{22}) + B_\Pi[J(J+1) - 1] - D_\Pi[J(J+1) - 1]^2 \quad (14)$$

$$W_{11} = qx + q_D x^2 \quad (15)$$

$$W_{31} = \frac{\sqrt{3}}{2}(q + q_D x)[(x-2)(x-6)]^{1/2} \quad (16)$$

$$W_{03} = K_{03}\,[x(x-2)(x-6)]^{1/2} \quad (17)$$

The *J*-dependence of W_{03}, which connects the Σ and Φ states, was determined by applying the $\hat{J}^{+3}$ operator (in the molecular frame) to the Φ state basis function. The purpose of this perturbation analysis was to obtain the unperturbed constants for the 001 (Σ_u^+) state, and to estimate the vibrational energy of the 03^30 (Φ_u) state.

All rotational lines of the 001 → 000, 002 → 001 and 200 → 001 bands were fitted using the Hamiltonian matrix in eqn. (11) for the 001 levels, while the constants of 000, 002 and 200 states were fixed to the values reported in Tables 1 and 2. Rotational constants (B, D) and the *l*-type doubling constants (q, q_D) of the 03^10 (Π_u) and 03^30 (Φ_u) states were fixed to the values estimated by extrapolating the 000, 01^10, 02^00 and 02^20 constants. The following expression was used to estimate the $B_{[v]}$ values as accurately as possible:[52]

$$\begin{aligned} B_{[v]} = {} & B_e - \alpha_1\left(v_1 + \tfrac{1}{2}\right) - \alpha_2(v_2 + 1) - \alpha_3\left(v_3 + \tfrac{1}{2}\right) \\ & + \gamma_{11}\left(v_1 + \tfrac{1}{2}\right)^2 + \gamma_{22}(v_2 + 1)^2 + \gamma_{33}\left(v_3 + \tfrac{1}{2}\right)^2 + \gamma_{ll}l^2 \\ & + \gamma_{12}\left(v_1 + \tfrac{1}{2}\right)(v_2 + 1) + \gamma_{13}\left(v_1 + \tfrac{1}{2}\right)\left(v_3 + \tfrac{1}{2}\right) \\ & + \gamma_{23}(v_2 + 1)\left(v_3 + \tfrac{1}{2}\right) \end{aligned} \quad (18)$$

Table 4 Spectroscopic constants (in cm^{-1}) for the observed rotational *l*-type resonance in $^{64}ZnD_2$

	State	B	$D/10^{-5}$	g_{22}	$q/10^{-2}$	$q_D/10^{-6}$	$G(02^21) - G(02^20)$
020	02^20 (Δ_g)	1.780 183(18)[a]	1.2633(20)	2.6491(47)	−2.0765(27)	0.440(24)	
	02^00 (Σ_g^+)	1.780 369(31)	1.2502(34)				
							1358.380 07(38)
021	02^21 (Δ_u)	1.764 886(19)	1.2597(22)	2.6340(47)	−2.0560(27)	0.423(23)	
	02^01 (Σ_u^+)	1.765 081(31)	1.2472(34)				

[a] All uncertainties are 1σ.

Table 5 Unperturbed constants (in cm^{-1}) for the 001 (Σ_u^+) states of $^{64}ZnH_2$ and $^{64}ZnD_2$

Constant[a]	$^{64}ZnH_2$	$^{64}ZnD_2$
$B(03^30)$	3.532 80[b]	1.778 78
$B(03^10)$	3.535 27	1.779 15
$10^5D(03^30)$	5.221	1.305
$10^5D(03^10)$	5.209	1.278
$10^2q(030)$	−5.949	−2.079
$10^6q_D(030)$	2.29	0.388
g_{22}	5.3811	2.6491
$G(03^30) - G(000)$	1906.1992(89)[c]	1378.3604(64)
$G(001) - G(000)$	1889.432 62(14)	1371.631 00(16)
$B(001)$	3.506 5923(23)	1.767 9993(16)
$10^5D(001)$	4.9254(9)	1.225 67(38)
$10^{10}H(001)$	4.44(9)	0.451(23)
$10^5K_{03}(\Sigma,\Phi)$	3.456(13)	0.672(14)

[a] The constants reported in this table can reproduce all the observed rotational energy levels of the 001 (Σ_u^+) states within their experimental uncertainties. [b] The constants B, D, q, q_D and g_{22} for the perturbing states (03^10 and 03^30) were fixed to the extrapolated values (see the text). [c] The numbers in parentheses are one standard deviation statistical uncertainties in the last quoted digits.

The above expression is preferred to eqn. (4) since it includes higher order terms. The constants γ_{22}, γ_{ll}, and $[-\alpha_2 + \gamma_{12} + \gamma_{23}]$ were obtained using the 000, 01^10, 02^00 and 02^20 $B_{[v]}$ values, and were used to calculate the $B_{[v]}$ constants of the 03^30 and 03^10 states of $^{64}ZnH_2$ and $^{64}ZnD_2$. A quadratic expression analogous to eqn. (18) was used to calculate the $D_{[v]}$ constants. For the minor isotopologues of ZnH_2 and ZnD_2, the γ_{22} and γ_{ll} constants were not available and the corresponding constants of $^{64}ZnH_2$ and $^{64}ZnD_2$ were used instead. The l-type doubling constants $q_{[v]}$ and $q_{D,[v]}$ were estimated using the corresponding constants of 010 and 020 levels, and by assuming a linear vibrational dependence, similar to eqn. (4), for these parameters. The vibrational constants g_{22} of ZnH_2 and ZnD_2 were also fixed to the values reported in Tables 3 and 4. The least-squares fitting resulted in determination of G_Φ (vibrational energy of the 03^30 state), K_{03} (off-diagonal matrix element between Σ and Φ states), and the unperturbed constants of the 001 (Σ_u^+) state for both $^{64}ZnH_2$ and $^{64}ZnD_2$ molecules (Table 5). The constants of Table 5 differ slightly from those reported in Tables 1 and 2 for the 001 (Σ_u^+) states. For example, since all the rotational lines (including high J's) were included in the perturbation analysis, the third order H_{001} constants were also required for both $^{64}ZnH_2$ and $^{64}ZnD_2$. Overall, the constants of Table 5 are more reliable for the 001 (Σ_u^+) states, because they reproduce all the observed energy levels within their experimental uncertainties (~ 0.001 cm^{-1}).

The Σ–Φ interaction constants (K_{03}) were determined to be $3.456(13) \times 10^{-5}$ cm^{-1} and $0.672(14) \times 10^{-5}$ cm^{-1} for $^{64}ZnH_2$ and $^{64}ZnD_2$, respectively. The off-diagonal matrix element W_{03} is zero for $J < 3$, and it increases rapidly with J. At the highest observed rotational levels of $^{64}ZnH_2$ ($J = 28$) and $^{64}ZnD_2$ ($J = 35$), W_{03} is about 0.8 cm^{-1} and 0.3 cm^{-1}, respectively. Although the vibrational energies of the 03^30 states (G_Φ) of $^{64}ZnH_2$ and $^{64}ZnD_2$ have statistical uncertainties of ~ 0.01 cm^{-1} in Table 5, we estimate an absolute accuracy of about 0.5 cm^{-1} for these energies, because several constants in our fits were fixed to the extrapolated values. The outputs of the least-squares fits and the corresponding constants for $^{66}ZnH_2$, $^{68}ZnH_2$, $^{66}ZnD_2$ and $^{68}ZnD_2$ have been placed in Table S9.†

A few rotational lines of the 01^11 (Π_g) states of both ZnH_2 and ZnD_2 were perturbed by the nearby 040 vibrational level, which has 04^00 (Σ_g^+), 04^20 (Δ_g) and 04^40 (Γ_g) states. In this case, it was not clear which states were causing the perturbations observed in e and f parity components of the 01^11 (Π_g) state. We tried to perform a similar perturbation fit for this state by estimating the constants of the 040 level, but we were unable to fit the e and f parity components together.

3.4. Fermi resonance

Ab initio calculations at the MP2, CCSD(T) and DFT(B3LYP) levels of theory[9,21] predicted that the vibrational frequencies of the symmetric stretching (ω_1) and antisymmetric stretching (ω_3) modes are very close to each other in both ZnH_2 and ZnD_2. In case of ZnD_2, ω_3 was predicted to be larger than ω_1 by about 30 cm^{-1}. This energy separation is smaller for ZnH_2, and in fact the results of MP2, CCSD(T) and DFT(B3LYP) calculations were inconsistent in determining which vibrational mode has the higher frequency.[9,21] The highest level calculation to date, CCSD(T) with a relatively large basis set, predicted that ω_1 is slightly larger than ω_3 for ZnH_2.[21]

There is no interaction between the 100 (Σ_g^+) and 001 (Σ_u^+) states, because they have opposite g/u symmetry. However, the 002 and 200 states have the same symmetry (Σ_g^+), and are strongly coupled due to Fermi resonance. We clearly observed the effects of this resonance in our ZnH_2 spectrum: (a) The zinc isotope shift in the 002 (Σ_g^+) → 001 (Σ_u^+) band of ZnH_2 was unusually small compared to all regular bands (see Fig. 4), which is an indication of mixing between 002 and 200 states; (b) The vibrational band origin of the 002 (Σ_g^+) → 001 (Σ_u^+) band of ZnH_2 was unusually high, which indicates that the rotational levels of the 002 (Σ_g^+) state are systematically shifted towards higher energies; (c) The $B_{[v]}$ value of the 002 (Σ_g^+) state was slightly different from the value predicted by α_3, which indicates that this state is mixed with another state with a different $B_{[v]}$ value; d) The 200 (Σ_g^+) → 001 (Σ_u^+) combination band that should be very weak in the absence of resonance appeared in our ZnH_2 spectrum, and it had a small zinc isotope shift in the opposite direction of those of all other bands.

The 002 (Σ_g^+) and 200 (Σ_g^+) states of ZnH_2 are pushed apart due to Fermi resonance. More precisely, rotational levels of the 002 (Σ_g^+) state are shifted towards higher energies, and those of the 200 (Σ_g^+) state are shifted towards lower energies by exactly the same amount. Therefore, for each value of J, the sum of their energies remains unchanged. It is straightforward to show that the sum of vibrational energies [$G_{sum} = G_{002} + G_{200}$], rotational constants [$B_{sum} = B_{002} + B_{200}$], and centrifugal distortion constants [$D_{sum} = D_{002} + D_{200}$] also remain unchanged. The effective $G_{[v]}$, $B_{[v]}$ and $D_{[v]}$ constants of the 002 (Σ_g^+) and 200 (Σ_g^+) states of $^{64}ZnH_2$ (Table 1) were used to

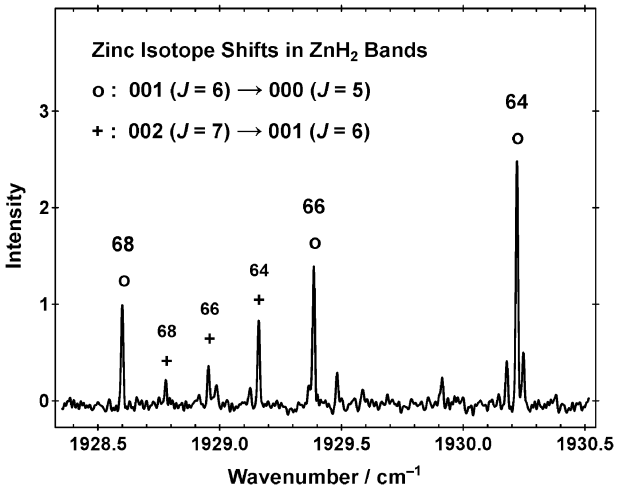

Fig. 4 An expanded view of the ZnH_2 spectrum showing the zinc isotope shifts in two R-branch lines. The zinc isotope shifts in the 002 → 001 hot band are unusually small, due to the coupling between 002 and 200 states (Fermi resonance).

calculate these sums. We performed a Fermi resonance fit for these states using the following 2 × 2 Hamiltonian matrix, which is similar to the one used for the 100 (Σ_g^+) and 02^00 (Σ_g^+) states of the CO_2 molecule:[49,53]

$$\boldsymbol{H} = \begin{pmatrix} E_\Sigma^0(002) & -K_{00} \\ -K_{00} & E_\Sigma^0(200) \end{pmatrix}. \quad (19)$$

The diagonal elements in the above matrix are simple energy expressions for the Σ states with $G_{[v]}$, $B_{[v]}$ and $D_{[v]}$ constants, and K_{00} is the perturbation matrix element that has no J-dependence. All rotational lines of the 002 → 001, 200 → 001 and 003 → 002 bands of ZnH_2 were fitted using the Hamiltonian matrix in eqn. (19) for the 002 and 200 states, and the constants of 001 and 003 states were fixed to the previously determined values (Tables 5 and 1, respectively). The sums of $G_{[v]}$, $B_{[v]}$ and $D_{[v]}$ constants for the 002 (Σ_g^+) and 200 (Σ_g^+) states, *i.e.*, G_{sum}, B_{sum} and D_{sum}, were also fixed to the values calculated from Table 1. In order to determine the off-diagonal matrix element (K_{00}) and the unperturbed constants for these states, we had to fix at least one more parameter in our fit. We chose to fix the D_{200} constant to the extrapolated value, *i.e.*, $D_{200} = 2D_{100} - D_{000}$, because the 000 ($\Sigma_g^+$) and 100 ($\Sigma_g^+$) states are not perturbed, and their $D_{[v]}$ constants are reliable. Since no rotational line with $J > 16$ was observed for the 100 (Σ_g^+) and 200 (Σ_g^+) states, we fitted only the low-J lines of the 001 → 000 band to obtain a comparable D_{000}, appropriate for extrapolation (see Table S1†). The constant D_{200} was then calculated to be 4.8891×10^{-5} cm^{-1}, and was held fixed in the least-squares fitting. Only three parameters, *i.e.*, G_{200}, B_{200} and K_{00}, were allowed to vary in the fit, and the results are presented in Table 6. The constants of the 002 (Σ_g^+) state were then calculated by subtracting G_{200}, B_{200} and D_{200} from G_{sum}, B_{sum} and D_{sum}, respectively. The constants of Table 6 can reproduce all the observed energy levels of the 002 and 200 states within their experimental uncertainties (0.001 or 0.002 cm^{-1}). The outputs of the least-squares fitting program and the corresponding constants for $^{66}ZnH_2$ and $^{68}ZnH_2$ are in Table S10.† The off-diagonal matrix element (K_{00}) was determined to be 28.168(7) cm^{-1}. The unperturbed G_{002} constant in Table 6 is about 19 cm^{-1} larger than G_{200}, but this energy separation increases to about 59 cm^{-1} (Table 1) due to the off-diagonal matrix element (K_{00}). Although the unperturbed G_{200} constant of $^{64}ZnH_2$ has an uncertainty of ~0.02 cm^{-1} in the fit (Table 6), we estimate an absolute accuracy of about 0.5 cm^{-1} for G_{002} and G_{200}, because the D_{200} constant in our fit was fixed to an extrapolated value.

The constants of Table 6 can be used to calculate the eigenfunctions for the 002 (Σ_g^+) and 200 (Σ_g^+) states from their basis functions, and to quantify the extent of mixing between the two states. The eigenfunctions of the perturbed states are related to their unperturbed basis functions by the following equations:[46]

$$|002',J\rangle = c_1|002,J\rangle - c_2|200,J\rangle \quad (20)$$

$$|2'00,J\rangle = c_2|002,J\rangle + c_1|200,J\rangle \quad (21)$$

In these equations, c_1 and c_2 are equal to cos θ and sin θ, respectively, and of course $c_1^2 + c_2^2 = 1$. For each value of J, the mixing coefficients c_1^2 and c_2^2 can be calculated using the following equation,[46] which relates θ to the matrix elements of eqn. (19):

$$\tan 2\theta = \frac{2K_{00}}{E_\Sigma^0(002) - E_\Sigma^0(200)}. \quad (22)$$

The mixing coefficients c_1^2 and c_2^2 were determined for $J = 0$ to 15 levels of the 002 (Σ_g^+) and 200 (Σ_g^+) states of $^{64}ZnH_2$. The extent of mixing decreases very slowly with increasing J; for example, there is a 66%–34% mixture at $J = 0$, and a 69%–31% mixture at $J = 15$. Similar calculations for $^{66}ZnH_2$ and $^{68}ZnH_2$ showed mixing almost to the same extent (see Table S11).† Therefore, the observed 002 (Σ_g^+) state of ZnH_2 can be considered approximately as a 2/3 : 1/3 mixture of the unperturbed 002 and 200 states, and *vice versa*.

Another way to quantify the mixing between these states is to consider the zinc isotope shifts for the 002 (Σ_g^+) → 001 (Σ_u^+) band. For the unperturbed bands of ZnH_2 in the ν_3 region, *i.e.*, $(v_1,v_2,v_3 + 1) \rightarrow (v_1,v_2,v_3)$, the observed ^{64}Zn:^{66}Zn isotope shift is about 0.8 cm^{-1}. In other words, ω_3 for $^{64}ZnH_2$ is larger than that of $^{66}ZnH_2$ by about 0.8 cm^{-1}. On the other hand, ω_1 has no dependence on the mass of zinc atoms within the harmonic oscillator approximation. Therefore, the ^{64}Zn : ^{66}Zn isotope shifts for the 002 (Σ_g^+) → 001 (Σ_u^+) and 200 (Σ_g^+) → 001 (Σ_u^+) bands are expected to be +0.8 and −0.8 cm^{-1}, respectively, in the absence of Fermi resonance. The observed ^{64}Zn:^{66}Zn isotope shift of the 002 (Σ_g^+) → 001 (Σ_u^+) band of ZnH_2 was about +0.2 cm^{-1}, which indicates that the observed 002 (Σ_g^+) state is approximately a 62%–38% mixture of the unperturbed 002 and 200 states, consistent with the more accurate results obtained from eqns. (20)–(22). The energy separation between ω_1 and ω_3 of ZnD_2 is larger than that of ZnH_2,[21] and the Fermi resonance effects in ZnD_2 were not as severe as in ZnH_2. We did not observe the 200 (Σ_g^+) → 001 (Σ_u^+) combination band for ZnD_2, because the extent of mixing between the 200 and 002 states is relatively small. In this case, the observed ^{64}Zn:^{66}Zn isotope shift was about 1.2 cm^{-1} for the unperturbed bands in the ν_3 region, and about 1.0 cm^{-1} for the 002 (Σ_g^+) → 001 (Σ_u^+) band. Based on the isotope shifts, we estimate that the observed 002 (Σ_g^+) state of ZnD_2 is approximately a 92%–8% mixture of the unperturbed 002 and 200 states. There is yet another way to estimate the mixing coefficients for the 002 and 200 states of ZnD_2. The effective B_{002} constant of $^{64}ZnD_2$ (observed) is related to the unperturbed B_{002}^0 and B_{200}^0 constants by the following equation:[47]

$$B'_{002}\ (\text{obs.}) \approx c_1^2 B_{002}^0 + c_2^2 B_{200}^0. \quad (23)$$

The unperturbed B_{002}^0 and B_{200}^0 constants of $^{64}ZnD_2$ were estimated using α_3 and α_1, respectively, and the effective B_{002} constant was taken from Table 2. The mixing coefficients, c_1^2 and c_2^2, were found to be 93% and 7%, respectively, consistent with the ones calculated from zinc isotope shifts.

Table 6 Unperturbed constants (in cm^{-1}) for the 002 (Σ_g^+) and 200 (Σ_g^+) states of $^{64}ZnH_2$

State	$G_{[v]} - G_{000}$	B	$D/10^{-5}$	K_{00} (Σ,Σ)
[002 + 200][a]	7485.262 40[a]	6.909 050[a]	9.7646[a]	
200 (Σ_g^+)	3733.334(21)[b]	3.444 130(16)[b]	4.8891[c]	28.1680(73)[b]
002 (Σ_g^+)[d]	3751.928[d]	3.464 920[d]	4.8755[d]	

[a] Sum of the effective constants for the 200 and 002 states, calculated directly from Table 1 and held fixed in the least-squares fitting (see the text). [b] These constants were determined by least-squares fitting. The numbers in parentheses are 1σ uncertainties in the last quoted digits. [c] D_{200} was calculated using D_{000} and D_{100} constants, and held fixed in the fit (see the text). [d] The unperturbed constants of the 002 state were finally calculated by subtracting G_{200}, B_{200} and D_{200} from G_{sum}, B_{sum} and D_{sum}, respectively (see the text).

3.5. Determination of bond lengths

The B_{000} constants of $^{64}ZnH_2$ and $^{64}ZnD_2$, taken from Tables 1 and 2, were used to determine the r_0 bond lengths directly from the moment of inertia equation. The r_0 values obtained for $^{64}ZnH_2$ and $^{64}ZnD_2$ are 1.535 274(2) Å and 1.531 846(3) Å, respectively. Their difference is in the fourth significant figure, and is due to the fact that the 000 ground state of ZnD_2 lies lower than that of ZnH_2 on the potential energy surface.

The vibration–rotation interaction constants (α_1, α_2 and α_3 in eqn. (4)) were determined by taking the differences between the ground state rotational constant (B_{000}) and the $B_{[v]}$ values of the 100, 01^10 and 001 states, respectively. The equilibrium rotational constant (B_e) was then calculated for both $^{64}ZnH_2$ and $^{64}ZnD_2$ using their B_{000} values and the three α's. The equilibrium constants of $^{64}ZnH_2$ and $^{64}ZnD_2$ determined in this study are listed in Table 7, and those for the minor isotopologues are in Table S12.† Although eqn. (18) for $B_{[v]}$ is more accurate than eqn. (4), we did not use it for calculation of B_e, because our experimental data are not sufficient for determination of some higher order constants in eqn. (18), *i.e.*, γ_{12} for both isotopologues and γ_{11} for $^{64}ZnD_2$. The equilibrium centrifugal distortion constant (D_e) was calculated in a similar way, using a linear equation analogous to eqn. (4) for the $D_{[v]}$ values.

Using the B_e values of 3.600 269(31) cm^{-1} and 1.801 985(25) cm^{-1} for $^{64}ZnH_2$ and $^{64}ZnD_2$, respectively, we obtained the equilibrium bond distances (r_e) of these isotopologues independently. The r_e values were determined to be 1.524 13(1) Å and 1.523 94(1) Å for $^{64}ZnH_2$ and $^{64}ZnD_2$, respectively. The difference in the r_e values of $^{64}ZnH_2$ and $^{64}ZnD_2$ is very small (only about 0.01%), but still considerably larger than the statistical uncertainties. This discrepancy appears to be due to the breakdown of Born–Oppenheimer approximation or the exclusion of higher order γ constants in determination of B_e. In order to examine the contribution of γ constants in this discrepancy, we recalculated the B_e constants of $^{64}ZnH_2$ and $^{64}ZnD_2$, this time from eqn. (18), by fixing the γ_{11} constant of $^{64}ZnD_2$ to the mass-scaled value and setting the unknown γ_{12} constants to zero. The new r_e values turned out to be 1.524 06(2) Å and 1.523 86(3) Å for $^{64}ZnH_2$ and $^{64}ZnD_2$, respectively, and their difference is still about 0.01%. Therefore, we believe that the main reason for this discrepancy is the breakdown of Born–Oppenheimer approximation.

In polyatomic molecules for which the available spectroscopic data are not sufficient to determine the equilibrium bond lengths, it is common to calculate the r_s structure by using the moments of inertia of isotopically substituted molecules.[54–57] For example, in our earlier paper on CdH_2 and CdD_2, we could not determine B_e and r_e due to the lack of data, and we used the B_{000} values of CdH_2 and CdD_2 together to obtain the r_s bond length.[37] We have determined both r_0 and r_e for the $^{64}ZnH_2$ and $^{64}ZnD_2$ molecules independently, and an average r_s bond length is not necessary. We calculated r_s for this molecule only to compare it with the r_0 and r_e values. The following equation was used to estimate the r_s bond length:[56]

$$I_0^D - I_0^H = 2r_s^2(m_D - m_H). \quad (24)$$

In this equation, I_0^D and I_0^H are the moments of inertia calculated from the B_{000} values of $^{64}ZnD_2$ and $^{64}ZnH_2$, respectively, and m_D and m_H are the atomic masses for deuterium and hydrogen. The r_s bond length calculated from eqn. (24) is 1.528 41 Å, which lies between the r_0 and r_e values, qualitatively consistent with the predictions of Watson[57] for the relative magnitudes of r_0, r_s and r_e.

We also performed *ab initio* calculations for the bond length of gaseous ZnH_2 using the Gaussian 03 program.[58] The 6-311++G(3df, 3pd) basis set was used at the HF, DFT(B3LYP), MP2, MP3, MP4(SDQ), CISD, CCD and QCISD levels of theory, and the computed r_e values were in the range of 1.516 Å to 1.574 Å. The MP4(SDQ) method predicted 1.530 Å for r_e, which was the closest value to the experimental equilibrium bond lengths. The results of these calculations are presented in Table S13.†

Table 7 Molecular constants of $^{64}ZnH_2$ and $^{64}ZnD_2$ (in cm^{-1})

Constant	$^{64}ZnH_2$	$^{64}ZnD_2$
B_{000}	3.548 214(9)	1.783 424(7)
r_0/Å	1.535 274(2)	1.531 846(3)
α_1	0.051 86(3)[a]	0.018 32(3)
α_2	0.005 31(1)	0.001 69(1)
α_3	0.041 62(1)	0.015 42(1)
B_e	3.600 269(31)	1.801 985(25)
r_e/Å	1.524 13(1)	1.523 94(1)
$D_e/10^{-5}$	4.870(9)	1.220(4)
$q_{010}/10^{-2}$	−5.946(2)	−2.074(1)
ν_3	1889.4326(2)	1371.6310(2)
x_{13}	−61.7764(5)	−31.3209(6)
x_{23}	−12.4657(3)	−6.6386(3)
x_{33}	−13.47(1)	−5.47[b]
ω_1 (σ_g)	1958[c]	1385[c]
ω_2 (π_u)	656[d]	474[d]
ω_3 (σ_u)	1959.72(2)	1404.87[b]
g_{22}	5.381(6)	2.649(5)

[a] The numbers in parentheses are one standard deviation statistical uncertainties, calculated by propagation of errors. [b] The constants x_{33} and ω_3 of $^{64}ZnD_2$ are uncertain by a few cm^{-1} (see the text). [c] Estimated from B_e and D_e, using eqn. (26). [d] Estimated from q_{010}, B_e and ω_3, using eqn. (27).

3.6. Vibrational analysis

A few anharmonicity constants in eqn. (2) were directly calculated from our experimental band origins. The x_{13} constant was obtained for $^{64}ZnH_2$ and $^{64}ZnD_2$ by taking the difference between the 101 → 100 and 001 → 000 band origins. Similarly, x_{23} constants were calculated by taking the difference between the 01^11 → 01^10 and 001 → 000 band origins. Furthermore, the difference between the 002 → 001 and 001 → 000 band origins is equal to $2x_{33}$ (see eqn. (2)), but the 002 state is perturbed by Fermi resonance. We used the unperturbed G_{002} (from Table 6) to calculate this difference for $^{64}ZnH_2$ and to obtain the x_{33} constant. In the case of $^{64}ZnD_2$, we had to use the slightly perturbed G_{002} from Table 2, and the calculated x_{33} constant is not reliable. All the hot bands of $^{64}ZnH_2$ and $^{64}ZnD_2$ had smaller origins compared to the ν_3 fundamental bands, and thus the x_{13}, x_{23} and x_{33} constants have negative values (see Table 7).

The equilibrium vibrational frequency of the antisymmetric stretching mode (ω_3) was calculated simply by

$$\nu_3 \text{ (obs.)} = G_{001} - G_{000} = \omega_3 + 1/2x_{13} + x_{23} + 2x_{33}, \quad (25)$$

which is derived from eqn. (2). The ω_3 values for $^{64}ZnH_2$ and $^{64}ZnD_2$ turned out to be 1959.72 cm^{-1} and 1404.87 cm^{-1}, respectively, the latter being uncertain by about 5 cm^{-1} due to the error in determination of x_{33} for $^{64}ZnD_2$. The equilibrium vibrational frequency of the symmetric stretching mode (ω_1) was estimated using Kratzer's equation, which applies to diatomic and symmetric linear triatomic molecules:[47]

$$D_e = \frac{4B_e^3}{\omega_1^2}. \quad (26)$$

Using the B_e and D_e constants of Table 7, we estimated ω_1 to be 1958 cm^{-1} and 1385 cm^{-1} for $^{64}ZnH_2$ and $^{64}ZnD_2$, respectively. Our results indicate that ω_3 is larger than ω_1 for both ZnH_2 and ZnD_2, and their difference is larger in ZnD_2. The

bending mode vibrational frequency (ω_2) was also estimated for $^{64}ZnH_2$ and $^{64}ZnD_2$ using the following equation for the *l*-type doubling constant:[53,59]

$$q_{010} = -\frac{2B_e^2}{\omega_2}\left(1 + \frac{4\omega_2^2}{\omega_3^2 - \omega_2^2}\right). \quad (27)$$

The ω_2 values estimated from eqn. (27) are 656 cm^{-1} and 474 cm^{-1} for $^{64}ZnH_2$ and $^{64}ZnD_2$, respectively, and the latter has a larger uncertainty due to the small error in calculation of ω_3 for $^{64}ZnD_2$.

We also computed the harmonic vibrational frequencies of all isotopologues of ZnH_2 with the Gaussian 03 program,[58] using HF, MP2 and DFT(B3LYP) methods with the 6-311++G(3df,3pd) basis set, and the results are shown in Table S13.† The values of 1915, 643 and 1927 cm^{-1} were obtained for ω_1 (σ_g), ω_2 (π_u), and ω_3 (σ_u) of $^{64}ZnH_2$, respectively, using the DFT(B3LYP) method. The corresponding frequencies for $^{64}ZnD_2$ were computed to be 1355, 462 and 1384 cm^{-1}, respectively, using the same method. These numbers differ slightly from the ones reported in ref. 9 because we used a tighter convergence criterion in the Gaussian 03 program.

The other constants in eqn. (2), *i.e.*, x_{11}, x_{12} and x_{22}, could not be determined from our data, and therefore, the absolute vibrational energies of the 100 (Σ_g^+), 01^10 (Π_u) and 02^20 (Δ_g) states are not known with experimental accuracy. However, the vibrational energies of the 200 (Σ_g^+) state of ZnH_2 and the 03^30 (Φ_u) state of both ZnH_2 and ZnD_2 (Tables 5 and 6) have reasonable accuracies, and may be used to estimate roughly the vibrational energies of the 100, 01^10 and 02^20 states.

4. Discussion

4.1. Isotope effects

For a symmetric linear triatomic molecule such as ZnH_2, the vibrational frequencies of different isotopologues are related by the following equations:[47]

$$\left(\frac{\omega_1^i}{\omega_1}\right)^2 = \left(\frac{m_H}{m_H^i}\right), \quad (28)$$

$$\left(\frac{\omega_2^i}{\omega_2}\right)^2 = \left(\frac{\omega_3^i}{\omega_3}\right)^2 = \left(\frac{m_H}{m_H^i}\right)\left(\frac{m_{Zn}}{m_{Zn}^i}\right)\left(\frac{M^i}{M}\right). \quad (29)$$

In these equations, m_H and m_{Zn} are atomic masses of hydrogen (or deuterium) and zinc, respectively, and M is the total mass of the molecule. We observed the ν_3 fundamentals for several isotopologues of ZnH_2, and we also estimated ω_1, ω_2 and ω_3 for $^{64}ZnH_2$, $^{66}ZnH_2$, $^{68}ZnH_2$, $^{64}ZnD_2$ and $^{66}ZnD_2$. The observed ^{64}Zn:^{66}Zn isotope shift for the ν_3 fundamental band of ZnH_2 is 0.837 cm^{-1}, which corresponds to a ratio of 1.00044 between the ν_3 fundamentals of $^{64}ZnH_2$ and $^{66}ZnH_2$. The ratio predicted by eqn. (29) is 1.00046, and the discrepancy is in the sixth significant figure. Similarly, the observed ^{64}Zn : ^{66}Zn isotope shift for the ν_3 fundamental band of ZnD_2 is 1.194 cm^{-1}, corresponding to a ratio of 1.00087 between the ν_3 fundamentals of $^{64}ZnD_2$ and $^{66}ZnD_2$, whereas a ratio of 1.00090 is predicted by eqn. (29). The observed ratio between the ν_3 fundamentals of $^{64}ZnH_2$ and $^{64}ZnD_2$ (Table 5) is 1.3775 and the predicted ratio from eqn. (29) is 1.3926. If we use the estimated ω_3 frequencies from Table 7 instead, the agreement becomes better and a ratio of 1.3950 is obtained. The observed H : D isotopic ratios for ω_1 and ω_2 (Table 7) are 1.4136 and 1.3849, respectively, and the predicted ratios from eqns. (28) and (29) are 1.4137 and 1.3926, respectively.

Simple isotopic relations exist for the B_e, α_1 and D_e constants of symmetric linear triatomic molecules. These constants are not sensitive to the mass of central atom, and in the case of ZnH_2 they should change only when hydrogen is substituted with deuterium. The mass dependences of B_e and α_1 are given in eqns. (5) and (6), and the mass dependence of D_e is easily obtained by combining eqns. (5), (26) and (28). The observed ratios between the B_e, α_1 and D_e constants of $^{64}ZnH_2$ and $^{64}ZnD_2$ are 1.9979, 2.8313 and 3.9912, respectively, whereas the predicted ratios are 1.9985, 2.8252 and 3.9939, respectively. The other constant for which a relatively simple mass dependence can be found is the *l*-type doubling constant (q). This constant is related to B_e, ω_2 and ω_3 constants *via* eqn. (27), and its mass dependence is obtained by combining eqns. (5), (27) and (29). The observed ratio between q_{010} constants of $^{64}ZnH_2$ and $^{64}ZnD_2$ is 2.8665 and the predicted ratio is 2.8680. Overall, the observed isotope effects are consistent with the theoretical predictions. The r_e values for all the isotopologues should be the same if the Born–Oppenheimer approximation is exact. We found that r_e values are the same for different isotopes of zinc, within their experimental uncertainties. However, the r_e values of $^{64}ZnH_2$ and $^{64}ZnD_2$ (Table 7) differ in the fifth significant figure, and this is mainly due to the breakdown of the Born–Oppenheimer approximation.

4.2. Relative stability of gaseous ZnH_2

Gaseous ZnH_2 has been predicted to have a slightly higher energy than the ground state Zn (g) + H_2 (g),[21] and there is a large barrier to insertion for ground state Zn atoms into the H–H bond. However, when zinc atoms are excited to the metastable ^3P state in the presence of an electrical discharge, they can insert into the H–H bond, leading to an exoergic production of gaseous ZnH_2. Breaking the first Zn–H bond in ZnH_2 requires a significant amount of energy, while the second bond (ZnH) can be broken by a small fraction of that energy.[36] We used a combination of experimental and theoretical data to calculate these bond energies:

$$ZnH_2\ (g) \rightarrow ZnH\ (g) + H\ (g), \quad (30)$$

$$ZnH\ (g) \rightarrow Zn\ (g) + H\ (g). \quad (31)$$

The best *ab initio* theoretical value for the heat of formation of gaseous ZnH_2 from zinc vapor and molecular hydrogen[21] is +7.6 kcal mol^{-1}, and the experimental values for dissociation energies of H_2 and ZnH are 103.3 and 19.6 kcal mol^{-1}, respectively.[60] Therefore, the dissociation energy of the first Zn–H bond in ZnH_2 is estimated to be 76.1 kcal mol^{-1}, nearly four times larger than that of the second bond. The relative energies of gaseous MH and MH_2 molecules (M = Zn, Be and Mg) are compared in a simple diagram in Fig. 5. The best *ab initio* theoretical values for the heats of formation of

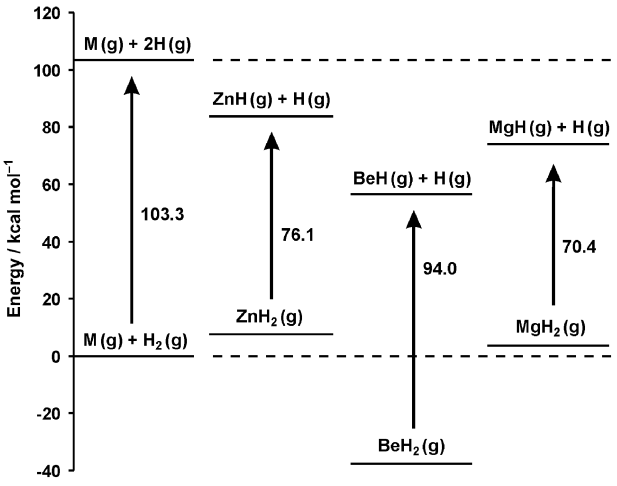

Fig. 5 A diagram showing the relative energies of gaseous metal monohydrides and dihydrides. For each metal (M), the energy of the ground state M (g) + H_2 (g) was taken as zero.

gaseous BeH_2 and MgH_2 from metal vapor and molecular hydrogen are −37.6 and +3.6 kcal mol^{-1}, respectively.[61,62] On the other hand, the experimental dissociation energies of BeH and MgH are 46.9 and 29.3 kcal mol^{-1}, respectively (see Fig. 5).[63,64] Therefore, the dissociation energies of the first metal–hydrogen bond in gaseous BeH_2 and MgH_2 are estimated to be 94.0 and 70.4 kcal mol^{-1}, respectively. Based on the energies required to break the first metal–hydrogen bonds, *i.e.*, MH_2 (g) → MH (g) + H (g), the order of stability is BeH_2 > ZnH_2 > MgH_2. It turns out that gaseous CdH_2 and HgH_2 (group 12) similarly lie between BeH_2 and MgH_2 in this series.[36,37] The other dihydrides of group 2 elements, *i.e.*, CaH_2, SrH_2 and BaH_2, have not been detected in the gas phase yet, and our efforts to generate these molecules have been unsuccessful.

5. Conclusions

High resolution infrared emission spectra of gaseous ZnH_2 and ZnD_2 in the ν_3 region were analyzed. The ν_3 fundamentals of the most abundant isotopologues, $^{64}ZnH_2$ and $^{64}ZnD_2$, were observed at 1889.433 cm^{-1} and 1371.631 cm^{-1}, respectively, and the band origins for the minor isotopes of zinc appeared at slightly lower wavenumbers, consistent with the theoretical predictions. In addition to the ν_3 fundamental bands of $^{64}ZnH_2$, $^{66}ZnH_2$, $^{67}ZnH_2$, $^{68}ZnH_2$, $^{64}ZnD_2$, $^{66}ZnD_2$ and $^{68}ZnD_2$, several hot bands involving ν_1, ν_2 and ν_3 were assigned and analyzed. Spectroscopic constants were obtained for each observed vibrational level by fitting the data to analytic energy level expressions. Rotational *l*-type doubling and *l*-type resonance, local perturbations, and Fermi resonances were observed in the vibration–rotation bands of both ZnH_2 and ZnD_2, and equilibrium vibrational frequencies (ω_1, ω_2 and ω_3) were estimated. Using the rotational constants of the 000, 100, 01^10 and 001 vibrational levels, the equilibrium rotational constants (B_e) of $^{64}ZnH_2$ and $^{64}ZnD_2$ were determined to be 3.600 269(31) cm^{-1} and 1.801 985(25) cm^{-1}, respectively, and the associated equilibrium bond lengths (r_e) were found to be 1.524 13(1) Å and 1.523 94(1) Å, respectively. The difference between the r_e values of $^{64}ZnH_2$ and $^{64}ZnD_2$ is about 0.01%, and is mainly due to the breakdown of the Born–Oppenheimer approximation.

Acknowledgements

Financial support for this project was provided by the Natural Sciences and Engineering Research Council (NSERC) of Canada.

References

1 G. D. Barbaras, C. Dillard, A. E. Finholt, T. Wartik, K. E. Wilzbach and H. I. Schlesinger, *J. Am. Chem. Soc*., 1951, **73**, 4585.
2 E. Wiberg, W. Henle and R. Bauer, *Z. Naturforsch*., 1951, **6b**, 393.
3 E. Wiberg, *Angew. Chem*., 1953, **65**, 16.
4 W. M. Mueller, J. P. Blackledge and G. G. Libowitz, *Metal Hydrides*, Academic Press, New York, 1968.
5 E. C. Ashby and J. J. Watkins, *Inorg. Synth*., 1977, **17**, 6.
6 D. F. Shriver, G. J. Kubas and J. A. Marshall, *J. Am. Chem. Soc*., 1971, **93**, 5076.
7 J. J. Watkins and E. C. Ashby, *Inorg. Chem*., 1974, **13**, 2350.
8 A. J. De Koning, J. Boersma and G. J. M. van der Kerk, *J. Organomet. Chem*., 1980, **186**, 159.
9 X. Wang and L. Andrews, *J. Phys. Chem. A*, 2004, **108**, 11006.
10 H. Smithson, C. A. Marianetti, D. Morgan, A. van der Ven, A. Predith and G. Ceder, *Phys. Rev. B*, 2002, **66**, 144107.
11 R. E. Linney and D. K. Russell, *J. Mater. Chem*., 1993, **3**, 587.
12 A. S. Luna, R. E. Sturgeon and R. C. de Campos, *Anal. Chem*., 2000, **72**, 3523.
13 R. E. Sturgeon and Z. Mester, *Appl. Spectrosc*., 2002, **56**, 202A.
14 S. Aldridge and A. J. Downs, *Chem. Rev*., 2001, **101**, 3305.
15 G. Simons and E. R. Talaty, *J. Chem. Phys*., 1977, **66**, 2457.
16 P. Pyykkö, *J. Chem. Soc., Faraday Trans. 2*, 1979, **75**, 1256.
17 J. Tyrrell and A. Youakim, *J. Phys. Chem*., 1980, **84**, 3568.
18 M. Kaupp and H. G. von Schnering, *Inorg. Chem*., 1994, **33**, 4179.
19 J. A. Platts, *J. Mol. Struct. (THEOCHEM)*, 2001, **545**, 111.
20 L. von Szentpály, *J. Phys. Chem. A*, 2002, **106**, 11945.
21 T. M. Greene, W. Brown, L. Andrews, A. J. Downs, G. V. Chertihin, N. Runeberg and P. Pyykkö, *J. Phys. Chem*., 1995, **99**, 7925.
22 D. Gullberg and U. Litzén, *Phys. Scr*., 2000, **61**, 652.
23 W. H. Breckenridge and J.-H. Wang, *Chem. Phys. Lett*., 1986, **123**, 17.
24 W. H. Breckenridge and J.-H. Wang, *J. Chem. Phys*., 1987, **87**, 2630.
25 W. H. Breckenridge and J.-H. Wang, *Chem. Phys. Lett*., 1987, **139**, 28.
26 J. M. Martínez-Magadán, A. Ramírez-Solís and O. Novaro, *Chem. Phys. Lett*., 1991, **186**, 107.
27 M. R. Salazar and J. Simons, *J. Chem. Phys*., 1996, **105**, 10919.
28 M. R. Salazar and J. Simons, *J. Chem. Phys*., 1999, **110**, 229.
29 W. H. Breckenridge, *J. Phys. Chem*., 1996, **100**, 14840.
30 L. Andrews, *Chem. Soc. Rev*., 2004, **33**, 123.
31 Z. L. Xiao, R. H. Hauge and J. L. Margrave, *High Temp. Sci*., 1991, **31**, 59.
32 V.A. Macrae, T. M. Greene and A. J. Downs, *J. Phys. Chem. A*, 2004, **108**, 1393.
33 V. A. Macrae, J. C. Green, T. M. Greene and A. J. Downs, *J. Phys. Chem. A*, 2004, **108**, 9500.
34 V. A. Macrae, T. M. Greene and A. J. Downs, *Phys. Chem. Chem. Phys*., 2004, **6**, 4586.
35 A. Shayesteh, D. R. T. Appadoo, I. E. Gordon and P. F. Bernath, *J. Am. Chem. Soc*., 2004, **126**, 14356.
36 A. Shayesteh, S. Yu and P. F. Bernath, *Chem. Eur. J*., 2005, **11**, 4709.
37 S. Yu, A. Shayesteh and P. F. Bernath, *J. Chem. Phys*., 2005, **122**, 194301.
38 H. Körsgen, P. Mürtz, K. Lipus, W. Urban, J. P. Towle and J. M. Brown, *J. Chem. Phys*., 1996, **104**, 4859.
39 H. Körsgen, K. M. Evenson and J. M. Brown, *J. Chem. Phys*., 1997, **107**, 1025.
40 H. Körsgen, W. Urban and J. M. Brown, *J. Chem. Phys*., 1999, **110**, 3861.
41 P. F. Bernath, A. Shayesteh, K. Tereszchuk and R. Colin, *Science*, 2002, **297**, 1323.
42 A. Shayesteh, K. Tereszchuk, P. F. Bernath and R. Colin, *J. Chem. Phys*., 2003, **118**, 3622.
43 A. Shayesteh, D. R. T. Appadoo, I. Gordon and P. F. Bernath, *J. Chem. Phys*., 2003, **119**, 7785.
44 A. Shayesteh, D. R. T. Appadoo, I. Gordon and P. F. Bernath, *Can. J. Chem*., 2004, **82**, 947.
45 A. G. Maki and J. S. Wells, *Wavenumber Calibration Tables from Heterodyne Frequency Measurements*, NIST Special Publication 821, U.S. Government Printing Office, Washington, 1991.
46 P. F. Bernath, *Spectra of Atoms and Molecules*, Oxford University Press, New York, 2nd edn., 2005.
47 G. Herzberg, *Molecular Spectra and Molecular Structure II. Infrared and Raman Spectra of Polyatomic Molecules*, Krieger, Malabar, FL, 1991.
48 G. Herzberg, *Rev. Mod. Phys*., 1942, **14**, 219.
49 D. M. Dennison, *Rev. Mod. Phys*., 1940, **12**, 175.
50 H. H. Nielsen, *Rev. Mod. Phys*., 1951, **23**, 90.
51 G. Amat and H. H. Nielsen, *J. Mol. Spectrosc*., 1958, **2**, 163.
52 A. G. Maki Jr. and D. R. Lide Jr., *J. Chem. Phys*., 1967, **47**, 3206.
53 D. Papoušek and M. R. Aliev, *Molecular Vibrational-Rotational Spectra*, Elsevier, Amsterdam, 1982.
54 J. Kraitchman, *Am. J. Phys*., 1953, **21**, 17.
55 C. C. Costain, *J. Chem. Phys*., 1958, **29**, 864.
56 A. Chutjian, *J. Mol. Spectrosc*., 1964, **14**, 361.
57 J. K. G. Watson, *J. Mol. Spectrosc*., 1973, **48**, 479.
58 M. J. Frisch, G. W. Trucks, H. B. Schlegel, G. E. Scuseria, M. A. Robb, J. R. Cheeseman, J. A. Montgomery Jr., T. Vreven, K. N. Kudin, J. C. Burant, J. M. Millam, S. S. Iyengar, J. Tomasi, V. Barone, B. Mennucci, M. Cossi, G. Scalmani, N. Rega, G. A. Petersson, H. Nakatsuji, M. Hada, M. Ehara, K. Toyota, R. Fukuda, J. Hasegawa, M. Ishida, T. Nakajima, Y. Honda, O. Kitao, H. Nakai, M. Klene, X. Li, J. E. Knox, H. P. Hratchian, J. B. Cross, V. Bakken, C. Adamo, J. Jaramillo, R. Gomperts, R. E. Stratmann, O. Yazyev, A. J. Austin, R. Cammi, C. Pomelli, J. W. Ochterski, P. Y. Ayala, K. Morokuma, G. A. Voth, P. Salvador, J. J. Dannenberg, V. G. Zakrzewski, S. Dapprich, A. D. Daniels,

M. C. Strain, O. Farkas, D. K. Malick, A. D. Rabuck, K. Raghavachari, J. B. Foresman, J. V. Ortiz, Q. Cui, A. G. Baboul, S. Clifford, J. Cioslowski, B. B. Stefanov, G. Liu, A. Liashenko, P. Piskorz, I. Komaromi, R. L. Martin, D. J. Fox, T. Keith, M. A. Al-Laham, C. Y. Peng, A. Nanayakkara, M. Challacombe, P. M. W. Gill, B. Johnson, W. Chen, M. W. Wong, C. Gonzalez and J. A. Pople, *GAUSSIAN 03, (Revision C.02)*, Gaussian, Inc., Wallingford, CT, 2004.

59 J. K. G. Watson, *Can. J. Phys.*, 2001, **79**, 521.
60 K. P. Huber and G. Hezberg, *Molecular Spectra and Molecular Structure IV. Constants of Diatomic Molecules*, Van Nostrand, New York, 1979.
61 J. M. L. Martin, *Chem. Phys. Lett.*, 1997, **273**, 98.
62 H. Li, D. Xie and H. Guo, *J. Chem. Phys.*, 2004, **121**, 4156.
63 R. Colin and D. De Greef, *Can. J. Phys.*, 1975, **53**, 2142.
64 W. J. Balfour and B. Lindgren, *Can. J. Phys.*, 1978, **56**, 767.

